

**EXPERIMENTAL STUDY ON INTERFACIAL TRANSITION ZONES
IN REINFORCED CONCRETE**

(Reprinted from the Journal of Materials, Concrete Structures and Pavements, JSCE,
No. 592/V-39, May 1998)



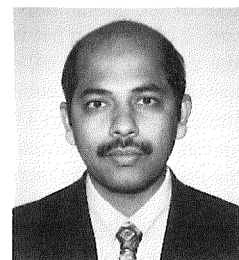
Nobuaki OTSUKI



Makoto HISADA



Nathaniel B. DIOLA



Tarek UDDIN Md.

This study compares the aggregate-matrix and steel bar-matrix interfacial transition zones (ITZs) with the purpose of determining their characteristics, differences, and the factors that affect them. The factors under consideration include the type of mineral admixture, the mix proportion, the steel bar orientation with respect to casting direction, and others. The results presented include a description of the ITZs and their properties. It is also shown that there is a great difference between the two ITZs, specifically with respect to the use of admixtures and gap formation under the aggregate or horizontal steel bars.

Keywords: *interfacial transition zone (ITZ), gaps, transition region, aggregates, reinforcing bars, corrosion*

Nobuaki Otsuki is a Professor at the Department of International Development Engineering at Tokyo Institute of Technology. He obtained his BS, MS, and D. Eng. degrees in Civil Engineering from the same institute. His main research interest is the durability of concrete structures.

Makoto Hisada is an Associate Professor at the Department of Civil Engineering and Architecture at Niigata University. He holds a D. Eng. in Civil Engineering from Tokyo Institute of Technology. His research interests include the migration of ions in concrete and the durability of concrete structures.

Nathaniel B. Diola is a doctoral student at Tokyo Institute of Technology where he received his MS in Civil Engineering in 1996. He holds a BS in Civil Engineering from the University of the Philippines in Diliman. His research interests include interfacial transition zones in concrete and the durability of concrete structures.

Tarek Uddin Md. is a Civil Engineer at the Overseas Civil Engineering Department of NEWJEC Inc. He obtained his D. Eng. from Tokyo Institute of Technology in 1997. His research interests include the corrosion of rebars in RC structures.

1. INTRODUCTION

The recent history of concrete use has illuminated an increasing number of new problems such as issues of durability and the need for a deeper understanding of concrete deeper has become urgent. Concrete, as viewed from a material science point of view, has thus become a lively subject of discussion. As advancements have been made in the field of material science, the study of concrete's individual components and their interactions has captured the attention of many researchers.

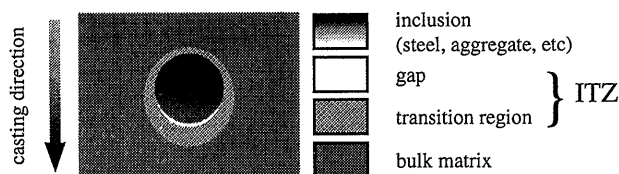


Fig. 1 Schematic representation of the ITZ

Studies of the interactions between aggregates and cement pastes in France (1948) revealed for the first time the existence of a region between the aggregate and the bulk paste with characteristics different from either material. At the time, this was called the “transition aureole” [1] though in recent literature it has evolved into the term “interfacial transition zone” (or ITZ). However, an exact definition of ITZ is hard to find in the literature. With reference to Fig. 1, an ITZ is defined in this paper as: *a region adjacent to any inclusion in concrete. It is composed of a gap, which may not be present at all times, and a transition region in which the matrix is affected by the presence of the inclusion.*

Until now, studies on ITZs have mainly considered aggregate-paste systems. In the case of steel-paste ITZs, investigations have been carried out using steel fibers/wires and also flat, polished steel surfaces. However, studies using reinforcing steel bars are scarce.

In this investigation, two ITZs were considered: namely that between aggregate and matrix and that between reinforcing steel bars and matrix. *Matrix* is a collective term used to refer to the paste, mortar, and concrete.

2. LITERATURE SURVEY

2.1 Introduction

Various investigations dealing with the ITZs under consideration are reviewed. It should be noted that previous studies on ITZs did not consider the existence of gaps. Hence, the term “ITZ” in these studies corresponds to “transition region” as previously defined.

2.2 The Aggregate-Paste ITZ

a) Formation Mechanism

Recent publications directly or indirectly support the “through solution” mechanism [2] of cement hydration as exemplified by Maso’s hypothesis [3,4]. This hypothesis explains the formation of hydration products but not the cause of the initial high water content or high porosity near the surface. To account for this, three mechanisms were proposed – namely the “wall effect” [3], the arch-shaped grain arrangement in contact with the aggregate [4], and the effect of vibration [6] but these still need verification by other researchers.

b) Morphology

Plain OPC Pastes: In general, the microstructure in the aggregate-paste transition region can be divided into two parts: an approximately 1 μm layer in contact with the aggregate and a paste region which may extend to some 50 μm or more and which is affected by the presence of the aggregate [5]. Some researchers [7,8] have shown that this thin layer is composed of CH and C-S-H and thus termed it a “duplex film”. Others [9,10] however detected only C-S-H. It was suggested that the reason for this lies in the aggregate properties, specifically the particle size [5]. It is important to note here that not all researchers were able to detect the “duplex film” [9,11].

The paste region affected by the presence of aggregate can be characterized as follows: 1) increasing porosity, CH, and C-S-H gradients and decreasing anhydrous cement content as the aggregate is approached [12]; 2) inherent weakness of this zone which causes microcracks to form here under any external stress [11]; and 3) formation of preferential fracture planes due to non-random orientation of the CH crystals which cleave easily along their basal plane [9].

Pastes with Mineral Admixtures: In a recent review, Bentur and Odler [13] summarized the effects of silica fume on the transition regions. The changes as compared with systems without silica fume include a reduction in transition zone thickness, a significant reduction in the amount of CH, especially after long hydration times, and a reduction in the preferential orientation of CH. These effects were attributed to both physical and chemical properties of silica fume. Due to its size, efficient packing near the interface can be achieved, and chemically, silica fume is highly pozzolanic and reacts to form C-S-H at the expense of $\text{Ca}(\text{OH})_2$.

Type F fly ash (5% cement replacement), when mixed with Portland cement, resulted in significant changes in the transition region structure [14]. In a study by Carles-Guibergues, et al. [quoted in 15], however, fly ash with porous grains reduced the zone size substantially while the use of fly ash from calcareous lignite or iron slag showed a tendency to increase the zone size.

Thickness of the Aggregate-Paste Transition Region: The ITZ, being a separate phase, should (at least hypothetically) have a volume or some dimension such as thickness. Determination of this 'thickness' has been an issue and values reported are dependent on the method of measurement and the definition of 'thickness' itself. For example, arguing from the view of particle packing and cement grain size, Scrivener [5] estimated the effective transition region thickness to be at least 50 μm , within which, a narrower band extending 20 μm from the aggregate has a more pronounced difference in properties as compared to the bulk paste. In another case, Snyder, et al. [quoted in 5] reported a value of 15~20 μm which is the range that best explains their MIP (Mercury Intrusion Porosimetry) data.

c) Transition Region Microhardness

Several authors have used microhardness measurements in the study of ITZs. Mindess [16] described the different problems encountered in microhardness testing, which include the use of very small loads in order to create small indentations, and the dependence of test results on the smoothness of the surface. Thus, hardness values obtained by various authors vary [as quoted in 16]: Mehta and Monteiro(1988) obtained ~1 kg/mm^2 ; Lyubimova and Pinus(1962) got 10-15 kg/mm^2 ; while Wang (1988) reported 10-30 kg/mm^2 .

d) The Aggregate-Paste ITZ as it Relates to Durability of Concrete Structures

It has been recognized that due to the inherent high porosity of the ITZ, it plays an important role in the durability of concrete, specifically in its transfer properties. Recent reviews have considered its effect on concrete's transfer properties [17] and the action of environmental conditions [18]. Suffice it to say that even though direct experimental evidence of the influence of the environment on the ITZs is limited, environmental factors affect the ITZ in the same way as they do in the bulk concrete. Improvements in the bulk concrete, such as mechanical strength are also accompanied by a reduction in porosity and permeability, though a generalization of the processes involved still faces technical as well as financial difficulties [18].

2.3 The Steel-Paste Interfacial Transition Zone

Investigations of the steel-paste ITZ can be divided into 3 categories depending on the form of the steel used: 1) *steel bar*, 2) *steel fiber/wire*, and 3) *steel plate*. Cases 1) and 3) can be classified as *fixed*, wherein movement of the steel during casting is restricted, as opposed to 2) in which the fiber/wire can move (*free*). This may lead to differences in the ITZ structure.

Most studies regarding this ITZ have focused on the second category while only very few used steel bars (category 1). The third category is mainly characterized by casting paste/mortar against a flat steel surface. In the following review, care will be taken to differentiate between the three.

a) Formation Mechanism

The formation mechanism of the transition region around steel fibers is taken to be similar to that around the aggregate [13]. The porous nature of the transition region is attributed to inefficient packing of cement particles due to the “wall effect” [4,5]. In the case of steel wires, the effect of vibration has been identified as one reason for the inefficient packing and resulting higher local W/C, and thus increased porosity, near the interface [6].

b) Morphology

Plain OPC Pastes: Studies on the ITZ between reinforcing steel bars and pastes have been scarce. With regard to morphology, Mindess [19] stated that it is similar to that of steel fiber-paste transition region. In a recent review, Bentur, et al. [14] pointed out that steel fiber-paste transition zone morphology is quite similar to that observed around aggregates in concrete. In effect, the reinforcing steel-paste transition region is similar to that of the aggregate-paste region. In general, the microstructure of the steel fiber-paste transition region can be characterized as being more porous than the bulk paste and rich in CH, which is mostly in contact with the fiber surface.

These observations point to the conclusion that the aggregate-paste and steel-paste ITZs are similar, but it will be shown later in this paper that there is a difference between them especially when interfacial gaps are considered.

Effect of Mineral Admixtures: Richness in CH is still observed even with the addition of admixtures. SEM observations reveal solid films of large CH crystals over most of the steel surface even in the presence of condensed silica fume (16% by weight) [20].

Thickness: As mentioned previously, the ‘thickness’ of the transition region as given in the literature depends on the actual definition of thickness and the measurement method. For the steel-paste ITZ case, an estimate of the thickness was provided by Wei, et al. [21] who reported the value to be 80 μm ; the point beyond which the microhardness of the paste around a steel-fiber became constant.

c) Transition Region Microhardness

Microhardness tests done by Wei, et al. [21], showed that microhardness values were lowest in the region around 25 to 35 μm from the surface of a 0.5mm fiber and that microhardness values fell with decreasing water to cement ratio.

d) Microstructure and Corrosion of Reinforcement

The kind of microstructure formed around the steel is of great importance as regards corrosion protection. Page [22] pointed out that the presence of CH in direct contact with the steel can modify the electrode characteristics of the metal. Since the CH film covers a considerable fraction of the metal surface, oxygen is screened and this also provides an alkaline buffer, which is necessary for passivation.

Monteiro, et al’s. study [20] on the effects of silica fume addition revealed that corrosion occurred only in silica fume-containing systems, and attributed this to the probably higher Cl:OH ratio in the pore solution. (They used composite specimens made by casting paste against a polished cross section of a 19 mm steel bar.) This is consistent with a previous study claiming that increasing the amount of silica fume reduced both the alkalinity and the chloride binding ability of the paste [23].

3. OBJECTIVES

In this investigation, ITZs were studied with the following two objectives: 1) To clarify the difference between the aggregate-matrix and steel-matrix ITZs if such a difference exists and 2) To identify and describe the general features of these ITZs.

4. EXPERIMENTAL PROCEDURE

4.1 Materials

a) Cement

A research-grade ordinary Portland cement provided by the Cement Association of Japan (CAJ) was used. Table 1 shows the chemical composition as well as the physical properties of this OPC together with those of the mineral admixtures used in this study.

b) Water

Tap water was used in all mixes.

c) Aggregates

Crushed sandstone coarse aggregate and ordinary river sand having the properties shown in Table 2 were used. Aggregates were washed during sieving, subsequently dried to approximately saturated-surface-dry (SSD) condition, and stored in sealed plastic containers prior to use to maintain the moisture content.

d) Mineral Admixtures

Fly ash (FA), blast furnace slag (BFS) and undensified silica fume (SF) were used as mineral admixtures. The properties of these admixtures are shown in Table 1.

e) Steel Bars

Round, plain, 6mm diameter steel bars (SR235) were used throughout the study. Their physical and chemical properties are shown in Table 3. Rust and other dirt on the surface were removed by polishing with #240 SiC abrasive paper. The steel pieces were then wiped thoroughly with a clean cloth and stored in a dessicator until casting.

4.2 Specimens

a) Specimens for Aggregate-Matrix ITZ Study

As shown in Table 4, seven mix proportions were used for the investigation. Cases 1-3 were all OPC pastes with varying W/C ratios. Common mineral admixture replacement ratios (FA: 30%, BFS: 50%, and SF: 10%) by volume were employed for cases 4-6, while case 7 corresponds to the paste part of a highly flowable concrete mix (OPC: 60%, BFS: 30%, and SF: 10%).

Mixing was done as follows: water and binder were mixed for 30s, stopped for 90s to remove paste adhering to the mixer wall, then the aggregates were added and mixing continued again for 120s. $\phi 100$ mm x 200 mm specimens (as shown in Fig. 2(b)) were cast. In all cases, placement was done in two lifts and each lift was

Table 1 Physical and chemical properties of ordinary Portland cement (OPC) and mineral admixtures

	OPC	FA	BFS	SF
Specific Gravity	3.14	2.18	2.89	2.24
Blaine Fineness, cm ² /g	3270	3240	8010	205500
Loss on Ig., %	0.60	1.74	1.20	1.38
SiO ₂ , %	21.30	50.71	32.30	97.50
Al ₂ O ₃ , %	5.30	24.12	13.80	0.41
CaO, %	64.40	10.01	41.50	0.19
MgO, %	2.20	2.20	6.80	0.29
SO ₃ , %	1.90	0.38	2.00	0.15
Na ₂ O, %	0.28	2.12	0.23	0.16
K ₂ O, %	0.60	1.25	0.33	0.37
TiO ₂ , %	0.37	1.29	1.47	0.00
MnO, %	0.10	0.00	0.34	0.17
Fe ₂ O ₃ , %	2.60	5.56	0.10	0.06
P ₂ O ₃ , %	0.20	0.00	0.00	0.05
C, %	0.01	0.67	0.00	0.00
S, %	0.00	0.00	0.00	0.00
Total, %	99.26	98.31	98.87	99.35

Table 2 Physical properties of aggregates

	Coarse Aggregate	Fine Aggregate
Specific Gravity (SSD)	2.65	2.62
Size, mm	4.7-9.7	<4.7
Absorption, %	0.681	-

Table 3 Physical and chemical properties of steel bars

Yield Point, N/mm ²	Tensile Strength, N/mm ²	C, %	Si, %	Mn, %	P, %	S, %
367	525	0.21	0.18	0.72	0.021	0.032

Table 4 Mix Proportions of aggregate-paste specimens

No.	Water - Binder Ratio W/B	Unit content (kg/m ³)						Slump [†] or Flow (cm)
		Water W	Cement C	Coarse Agg.* G	Mineral Admixture			
					FA	BFS	SF	
1	0.3	274	912	1154	-	-	-	9.2 [†]
2	0.5	386	772	976	-	-	-	70.0
3	0.7	468	668	846	-	-	-	75.0
4	0.5	363	560	1012	167	-	-	52.5
5	0.5	376	392	992	-	361	-	39.5
6	0.5	379	702	987	-	-	56	40.0
7	0.5	373	472	997	-	217	57	31.5

*Size of coarse aggregate: 4.7-9.7mm

Aggregate/binder ratio is 1.5 by volume for all cases

vibrated for one minute on a vibration table. After casting, the specimens were cured for 24 hours in an enclosure at 90%+ relative humidity. After demolding, the specimens were kept in curing cabinets controlled at 20°C, 30°C, and 60°C until the day of testing.

In designing the mix proportions, the water/binder and aggregate/binder ratios were fixed and thus, the slump or flow was not controlled.

b) Specimens for Steel-Matrix ITZ Study

The mix proportions are shown in the Table 5. These are similar to the ones listed in Table 4 except for the exclusion of the aggregate.

Horizontal and vertical steel bar orientations were considered in this study. In the case of horizontal bars, holes slightly larger than $\phi 6$ mm were drilled at the 50 mm and 150 mm marks from the bottom of standard $\phi 100$ mm x 200 mm mold cans. Steel bars were then inserted and the joints sealed with epoxy to retain the water during casting. On the other hand, in the vertical case, steel bars were set in the middle of $\phi 50$ mm x 100 mm molds. (see Fig. 2(a)). Curing was the same as for the aggregate-paste specimens.

c) Specimens for Comparing Aggregate-Matrix and Steel-Matrix ITZs

The specimen configuration was the same as that for steel-paste investigation, except for an additional “aggregate bar” (see Fig. 3(a)) placed such that its underside was at almost the same depth as the steel bar’s underside. These “aggregate bars” were fabricated by setting aggregates in epoxy.

Also, aggregates were included in the mix together with “floating steel” (Fig. 3(b)). “Floating steel” consisted of a $\phi 6$ mm x 10 mm long polished steel bar attached to a 10 mm x 10 mm x 5 mm styrofoam prism. The styrofoam was sized such that the unit weight of the “floating steel” was approximately equal to that of an aggregate particle (2.65). The mix proportions used are shown in Table 6.

4.3 Sample Preparation Procedures

a) Cutting

From the specimens shown in Fig. 2, bars containing the ITZ to be tested were cut using a diamond cutter. These bars were then cut crosswise by means of an ISOMET™ Low Speed Saw set at about 200 rpm. Water was used

Table 5 Mix proportions of steel-paste specimens

No.	Water-Binder Ratio W/B	Unit content (kg/m ³)					Flow (cm)	Bleeding Rate (%)
		Water W	Cement C	Mineral Admixture				
				FA	BFS	SF		
1	0.3	485	1617	-	-	-	18.8	0
2	0.5	611	1222	-	-	-	>30.0	8.12
3	0.7	687	982	-	-	-	>30.0	19.89
4	0.5	587	905	271	-	-	28.5	9.58
5	0.5	601	626	-	576	-	22.3	2.19
6	0.5	604	1119	-	-	89	24.8	3.16
7	0.5	598	757	-	348	91	21.3	1.74

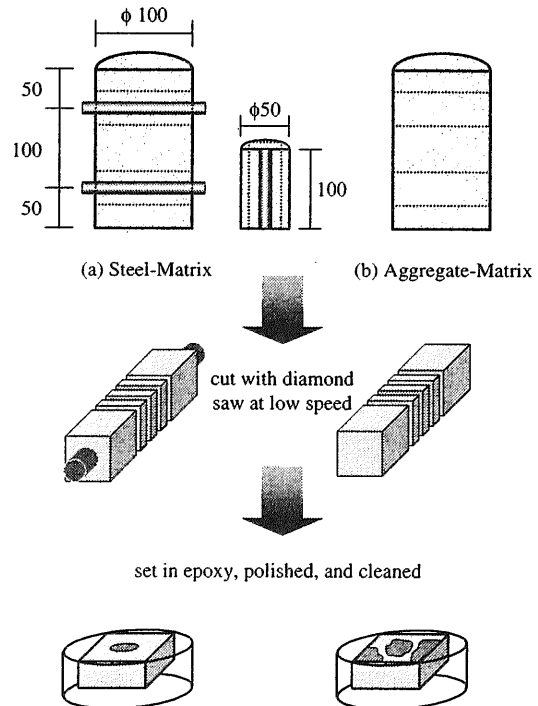


Fig. 2 Specimen configuration (unit: mm)

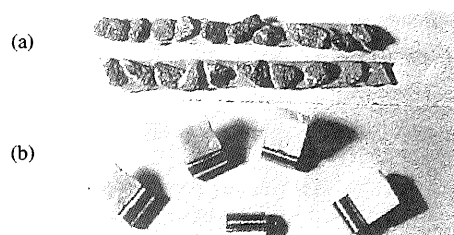


Fig. 3 a) aggregate bars and b) floating steel

as a coolant during the cutting process. To remove dirt after cutting, the specimens were cleaned using an ultrasonic cleaner. Since the succeeding procedures would take time, samples were stored in acetone to stop hydration.

In preparing the aggregate-matrix specimens for microhardness testing, difficulty was encountered in making sure that the section really showed the lowermost portion of the aggregate. Thus, for each aggregate under consideration, three sections were cut and from these, one was chosen, processed, and tested.

b) Setting in Epoxy

In order to avoid damage or specimen breakage during polishing, samples were set in an epoxy compound (Buehler's Epoxide Resin and Epoxide Hardener).

c) Polishing

After the epoxy had hardened, the samples were polished successively with SiC abrasives and finally with diamond paste (3 μm diamond particles) in a METASERV® 2000 Grinder and Polisher.

Again, after polishing, the samples were cleaned in an ultrasonic cleaner and subsequently stored in a desiccator until the time of testing. It was deemed necessary to store the polished specimens for microhardness testing under the same humidity and temperature conditions since the amount of moisture might affect the test results.

4.4 Methods

a) The Vickers Microhardness Test

A Vickers indenter was used and the test was performed as shown in Fig. 4. The diagonals (d_1 and d_2) were measured and the average was taken. Using the average diagonal and knowing the angle of inclination of the indenter faces, the contact surface area was calculated. Then the hardness, which is defined as the ratio of the applied load to the contact surface area, was obtained. Testing was done using a 10 gram-force load (the smallest possible for the machine used) with a 10-second contact time.

It should be noted that for measurement points close to each other, that there was a danger the indentations might overlap, which would not give the true hardness value. This was avoided by taking the measurements along a zigzag line. Care was taken to confirm the distance between measurement points from the face of the inclusion and that the distance between adjacent indentations was at least twice the average diagonal. Two specimens for each case were tested and each point plotted in the (shown later) is the average of at least three values.

b) Scanning Electron Microscopy

Previously cut composite bars (taken approximately 50 mm from the base of specimens), which had been stored in acetone, were dried in an oven at 100°C for 1 day and cooled down to room temperature. These were then fractured with a chisel and hammer. Caution was taken to avoid contact between the chisel and the location to be

Table 6 Mix proportions of specimens used in comparing steel-paste and aggregate-paste ITZs

No	W/ B	Unit content (kg/m ³)						M [†] (%)	Flow (cm)
		W	C	S	G	FA	SF		
1	0.3	274	912	-	1154	-	-	-	9.2 [‡]
2	0.5	386	772	-	976	-	-	-	70.0
3	0.7	468	668	-	846	-	-	-	75.0
4	0.5	363	560	-	1012	167	-	-	52.5
5	0.5	379	702	-	987	-	56	-	40.0
6	0.5	379	702	-	987	-	56	1.5	44.5
7*	0.5	386	771	386	586	-	-	-	74.0
8*	0.5	379	702	390	592	-	56	-	53.5
9*	0.5	379	702	390	592	-	56	1.5	56.0

Notes: 1) Refer to Tables 4 or 5 for definition of symbols
 2) Aggregate/binder ratio is 1.5 by volume for all cases
 *Sand/aggregate ratio is 0.4
[†] Chemical admixture (Mighty 150), % of binder by weight
[‡] Slump

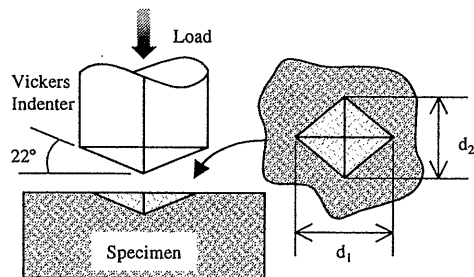


Fig. 4 The Vickers microhardness test

observed. Fracture surfaces were subsequently coated with carbon for the SEM examinations.

c) Visual Observation and Other Optical Methods

Macroscopic features such as the presence of large pores were observed and photos were taken for documentation. These photos were used as aids in describing the appearance of paste surfaces in contact with the steel or aggregate.

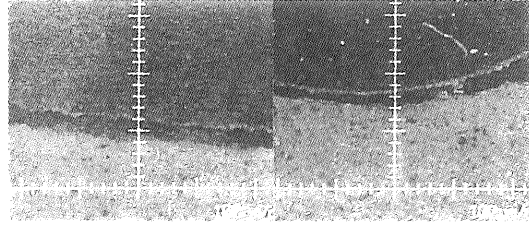


Fig. 5 Gap measurement using an optical microscope

In some specimens, gaps were observed under the horizontal steel bars and aggregates. The widths of these gaps were measured with an optical microscope and a scale of 100 μm per division was used. This is illustrated in Fig. 5 for the steel-paste and aggregate-paste cases.

4.5 Notes on Observation Procedure

Figure 6 defines the terms used in the discussion that follows. Note the difference between the use of the terms "under" and "lower". The former refers to the region below an inclusion while the latter refers to the location of the inclusion, which is 50 mm from the base of the specimen.

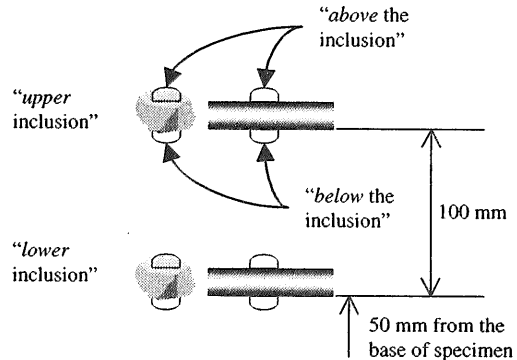


Fig. 6 Meaning of terms used in the discussion

In comparing the vertical and horizontal steel bars with respect to microhardness, the $\phi 50\text{ mm} \times 100\text{ mm}$ specimens with centrally located vertical steel bars were cut at the 50 mm mark from the base of the specimen. The transition regions above and below the lower horizontal bars were used for comparison.

5. THE AGGREGATE-PASTE ITZ

5.1 Introduction

Experimental results and discussions related to the aggregate-paste ITZs are presented and discussed with respect to a) transition region properties, which include thickness and microhardness, and b) gaps formed under the aggregate particles. The objective of this section is to describe the ITZ and some of its characteristics.

5.2 Discussion of Factors

a) W/C

The effect of W/C is first explained using the microhardness test results, as shown in Fig. 7. Measurements were taken in the paste region *above the aggregate* located 150 mm from the base of the specimens. The general trend is that the higher the W/C is, the lower are the microhardness values. It is also observed that the microhardness generally become lower as the aggregate surface is approached.

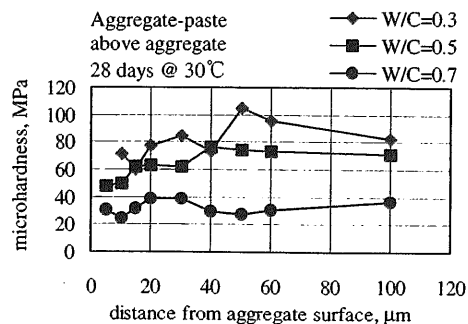


Fig. 7 Microhardness of aggregate-paste transition region

The point at which the hardness values started to

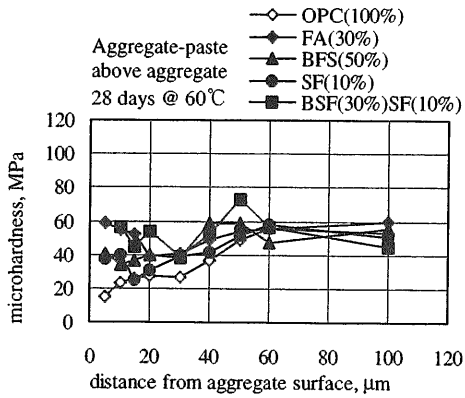


Fig. 8 Effect of mineral admixtures on the microhardness of the transition region

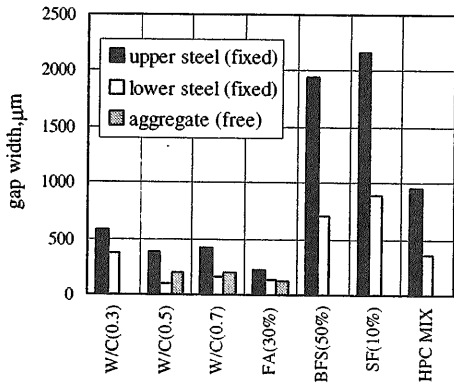


Fig. 9 Gaps under inclusions (paste case)

decrease as the aggregate is approached is designated as the upper limit of transition region thickness. For the cases under consideration, these points are not distinct. Looking at the general trend, however, for the case of $W/C = 0.3$ this point can be taken to be around $50 \mu\text{m}$, with $40 \mu\text{m}$ for $W/C = 0.5$ and $20 \mu\text{m}$ or less for $W/C = 0.7$. Thus, as W/C increases, the ITZ thickness decreases. This suggests that increasing the W/C makes both the transition region and the bulk matrix softer and the microhardness distribution near the aggregate becomes more uniform.

b) Mineral Admixtures

It can be observed from Fig. 8 that the microhardness values of cases with mineral admixtures lie above that of the control (100% OPC, $W/C=0.5$) especially near the aggregate surface. However, at points far from the aggregate surface the values are almost the same. Thus, in terms of microhardness, the addition of mineral admixtures makes the transition region ($< 50 \mu\text{m}$) harder but does not affect the bulk matrix significantly.

Another effect of mineral admixtures is in the size of the gaps formed under the aggregate. Compared to the control (100% OPC, $W/C=0.5$), it can be seen from Fig. 9 that the addition of admixtures reduces the gap size, as in the case of fly ash, or totally eliminates the gaps. Probable reasons for this phenomenon are discussed in Section 7.

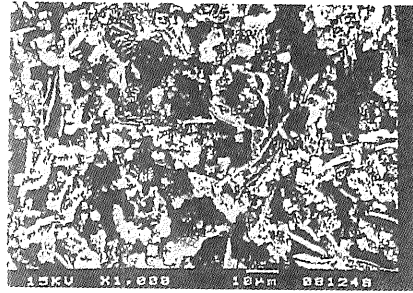


Fig. 10 SEM photo (100% OPC, $W/C=0.5$)



Fig. 11 SEM photo (90% OPC, 10% SF $W/B=0.5$)

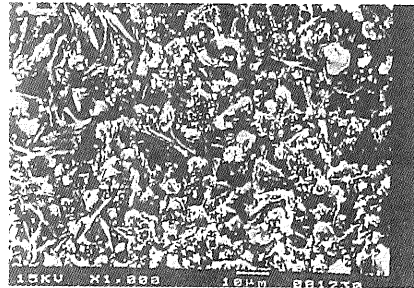


Fig. 12 SEM photo (60% OPC, 30% BFS, 10% SF, $W/B=0.5$)

As for SEM observations, Figs. 10-12 show the paste side of the fracture surfaces. These were the surfaces formerly in contact with the aggregates and since these were the surfaces where fracture occurred, these can be thought of as the weakest surfaces.

Taking Fig. 10 as the reference, the effect of admixture addition was to improve the transition region by making it denser. The pores (black spots) and hydration products are smaller in Figs. 11&12.

c) Location

Figure 13 compares the transition region microhardness measured *above* and *below* the aggregate. It is observed that of the 7 aggregate-paste systems considered, gaps formed under the aggregate in 3 cases (see Fig. 9): a) 100% OPC, W/C = 0.5; b) 100% OPC, W/C = 0.7; and c) 30% Fly Ash, W/B = 0.5. Figure 13(a) is a representative case in which no gaps formed. For these cases, there was no significant difference between the transition region microhardness above and below the aggregates. For those with gaps, however, (Fig. 13(b)) the presence of gaps under the aggregate led to lower microhardness at the lower transition region. The development of gaps below the aggregate is a very important subject and is discussed further toward the end of this paper.

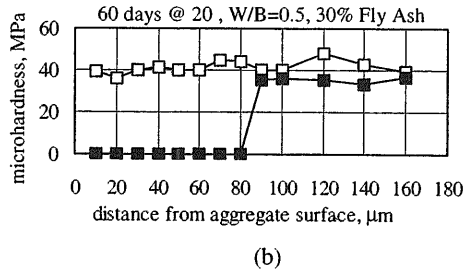
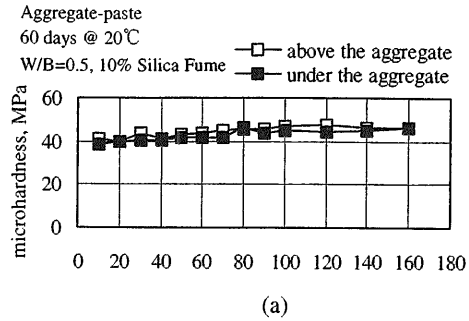


Fig. 13 Comparison of microhardness with respect to location: (a) zero gap case (b) with gap case

6. THE STEEL-PASTE ITZ

6.1 Steel Orientation

Steel orientation is defined with respect to casting direction. Horizontal bars and vertical bars refer to steel bars perpendicular and parallel to the casting direction, respectively. The main difference between the two lies in the nature of the paste surfaces at or near the steel surface.

a) Physical Description

Figure 14 shows representative crosssections of specimens with horizontal and vertical steel bars. The paste surrounding the steel bar in the vertical case is in continuous contact with the steel bar. On the other hand, only the upper paste portion is in contact with the horizontal steel bar. A large gap under the horizontal steel bar is clearly visible.

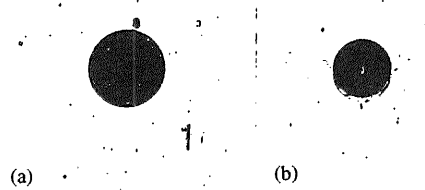


Fig. 14 Section across a (a) vertical bar and (b) horizontal bar (100% OPC, W/C = 0.5, 28 days @ 20°C)

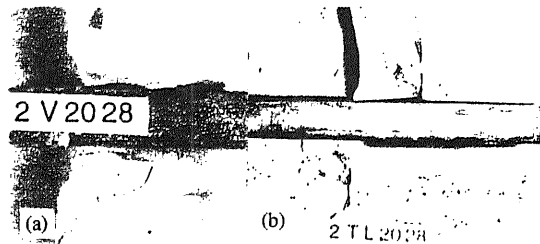


Fig. 15 Surface in contact with (a) vertical bar and (b) horizontal bar (100% OPC, W/C = 0.5, 28 days @ 20°C)

After breaking the specimens lengthwise, the paste surfaces were observed and representative surfaces are shown in Fig. 15. The paste surface in contact with the vertical steel bar is consistently smooth. However, large pores and rough surfaces (lower right of Fig. 15(b)) characterize the paste surface under the horizontal bar. Since the soundness of the matrix covering the steel is important in corrosion protection, the underside of horizontal steel bars in reinforced concrete may be a critical area.

b) Mechanical Difference

Microhardness measurements taken in the vicinity of steel bars located 50 mm above the base of specimens are shown in Fig. 16. Gaps were present under the horizontal bars and the microhardness of these gaps is designated as zero. It is observed that that the microhardness in the transition region around the vertical bars is comparable to that on top of the horizontal bars. However, the presence of gaps led to lower microhardness values under the horizontal bars.

6.2 Steel Position

Comparing horizontal bars placed at different depths (with upper bars 10 cm higher than lower bars), the gaps formed under lower bars were narrower. Table 7 shows the thickness of gaps under the horizontal bars for three W/C ratios. A discussion about these gaps will be presented in Section 7.

From these results it can be said that, as the height of the horizontal bar above the base of the specimen increases, the ITZ quality deteriorates and this may be an important point to consider in deciding the maximum height of a lift during concrete casting.

6.3 W/C

As shown in Table 7, W/C is not directly related to gap size. This observation also holds true for concrete, as will be discussed later. This may be attributed to a combination of factors, such as bleeding and autogeneous shrinkage, which are outside of scope of the present investigation.

In the case of transition region microhardness, specimens with low W/C were harder as shown in Fig. 17. (Note: from here on, microhardness values are those of the transition regions near vertical steel bars unless otherwise specified.)

Figure 18 shows representative pictures of paste surfaces formerly in contact with vertical steel bars. While it is true that the hydration products tend to be smaller and the morphology more compact as W/C decreases, it is observed that for the case of W/C = 0.5 and 0.7, the structures are comparable.

6.4 Mineral Admixtures

As for the microhardness results, Fig. 19 shows that except in the case of fly ash, the addition of admixtures led to a more uniform microhardness distribution. The values to the right of the 60 μm mark, which can be taken as those of the bulk paste, do not vary much from those to the left (transition region), in contrast with the case of OPC only and the case with fly ash. It can be concluded that this is due to the physical properties of the admixture. Fly ash, having a fineness of same magnitude as OPC, did not lead to a transition zone modification as compared to the other admixtures which have larger fineness values.

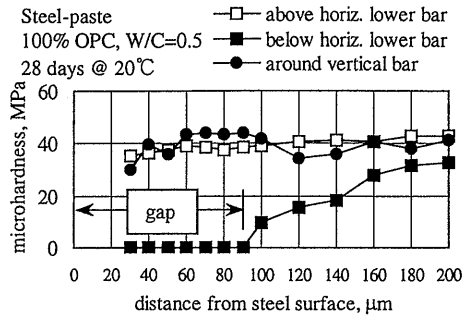


Fig. 16 Comparison between transition region microhardness of horizontal and vertical bars

Table 7 Gap sizes below upper and lower bars (paste case)

W/C	Upper Bar μm	Lower Bar μm	Upper Bar Gap/Lower Bar Gap
0.3	587	373	1.6
0.5	381	114	3.3
0.7	422	158	2.7

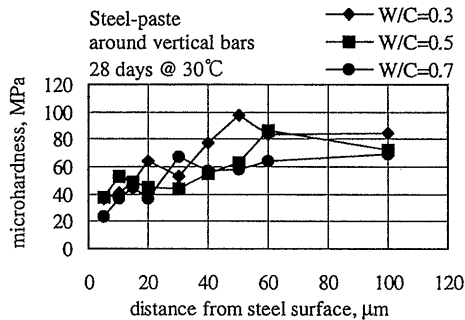


Fig. 17 Microhardness of the steel-paste transition region

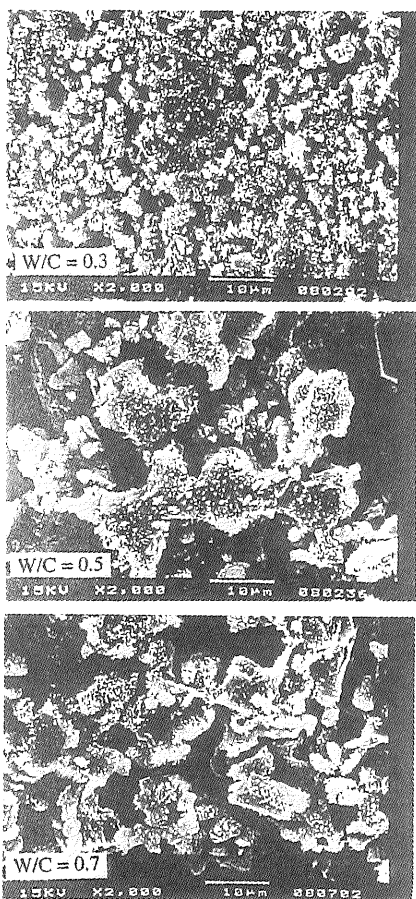


Fig. 18 SEM photos of paste in contact with the steel (28 days @ 20°C)

6.5 Extension of Steel-Paste Study to Reinforced Concrete

The same trends were observed for both paste and concrete specimens in relation to steel bar orientation (vertical vs. horizontal), steel bar location (upper vs. lower), and W/C. These can be summarized as 1) paste/concrete surfaces in contact with vertical bars and above upper horizontal bars were smooth while rough surfaces characterized by visible voids were observed at paste/concrete surfaces below horizontal bars; 2) gaps formed under upper bars were wider than those under lower bars; and 3) the W/C=0.3 case resulted in the widest gaps (Tables 7 and 8).

An interesting observation can be made with regard to corrosion. It is common knowledge that the rate of reinforcement corrosion depends on the migration of harmful substances at the interface. A compact ITZ means more protection from corrosion. Figure 20 shows steel bars and concrete surfaces taken from specimens with 10kg/m³ NaCl added to the concrete mix and cured at room temperature at around 90% RH for 6 months. The vertical steel bar show no visual signs of corrosion. In the case of horizontal steel bars, however, the lower surfaces are corroded while the top parts are uncorroded. With respect to steel bar location, the lower face of the upper bars corroded more than that of lower bars.

In summary, steel bars with sound ITZs showed no or little corrosion while those with gaps were all corroded. From this it can be said that, to protect steel bars from corrosion, not only should the transition region be strengthened or densified, but also gaps should be eliminated or at least minimized.

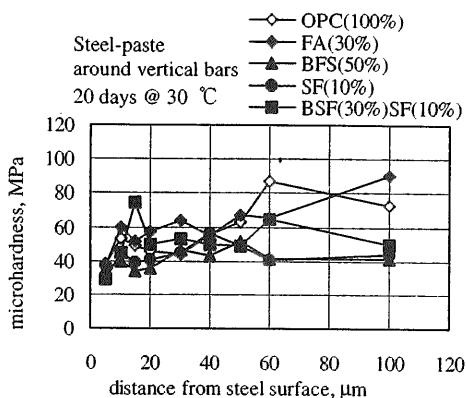


Fig. 19 Microhardness of the vertical steel-paste transition region for systems with mineral admixtures

Table 8 Gap sizes below upper and lower bars (concrete case)

W/C	Upper Bar Gap, µm	Lower Bar Gap, µm
0.4	400	0
0.5	200	0
0.7	200	0

With regard to the gaps under horizontal steel bars, it can be seen from Fig. 9 that except in the case of fly ash, the addition of mineral admixtures resulted in larger gaps. This result contrasts with that for aggregates, where the addition of mineral admixtures reduced or eliminated the gaps. A more detailed discussion of the differences between aggregate-matrix and steel-matrix ITZs will be presented in the next section.

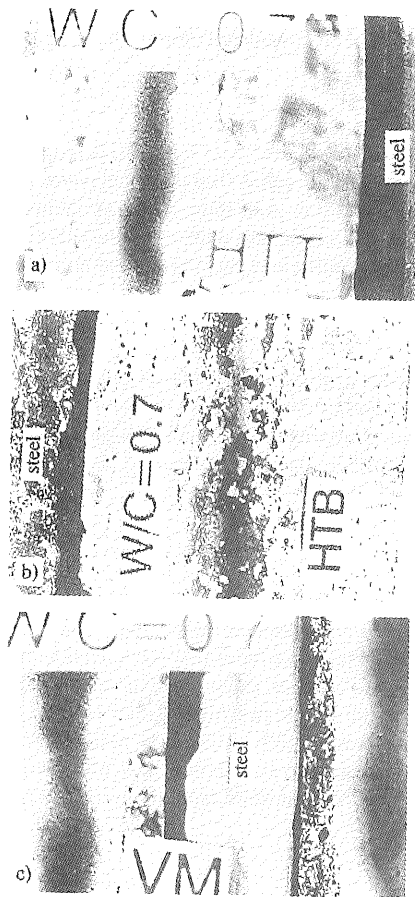


Fig. 20 Steel and concrete surfaces
a) above horizontal bar, b) below horizontal bar,
and c) vertical bar

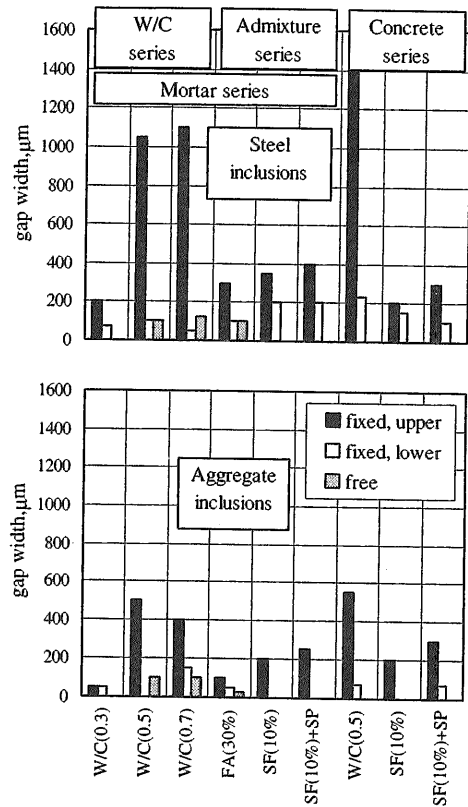


Fig. 21 Gaps under inclusions

7. COMPARATIVE STUDY BETWEEN THE AGGREGATE-MATRIX AND STEEL-MATRIX ITZ

7.1 Introduction

In the literature, studies on ITZs were concentrated on particular ITZs only. In this study, an attempt to compare the two ITZs was made, and this led to some interesting results. The comparison was made with respect to both gaps and transition regions.

7.2 Discussion of Gaps

a) Formation of Gaps

It has been observed that large gaps formed under horizontal steel bars (Tables 7 & 8). The presence of these gaps may critically affect both strength and durability. However, in the case of aggregates, gaps were found in only three mixes: that of W/C=0.5 and 0.7 using OPC and W/B=0.5 utilizing fly ash at a 30% replacement ratio. From Fig. 21, it is seen that the widest gap in the aggregate case was an order of magnitude narrower than that in the horizontal steel bar case. This phenomenon is thought to be caused by a difference in the relative movement of *inclusions* (hereafter used to refer to both steel bars and aggregate) with respect to the paste matrix. In order to validate this, an experiment with fixed and free inclusions was carried out, as described earlier. It should be noted however that in the case of fixed/free aggregate particles and free steel inclusions, specimen preparation

was difficult, so the observed sections may not accurately reflect the true gap width. However, by making careful selections from a number of sections, the results shown in Fig. 21 can be considered close to the true gap widths.

b) Fixed vs. Free Inclusions

As can be seen in Fig. 21, in almost all cases, larger gaps formed under fixed steel bars compared to free ones. This was also confirmed for the aggregate case. A possible explanation is that fixing an inclusion, particularly against the formwork, may lead to more vibration of the matrix around it. And thus, fixing an inclusion during casting may lead to the formation of gaps under it. This observation is consistent with a previous study [6] where it was noted that vibration can lead to higher local water content and inefficient packing around an inclusion.

c) Gaps and Inclusion Surface Conditions

It was observed that, in all cases considered, the gaps formed under aggregate particles are equal to or smaller in size than those formed under corresponding steel, regardless of whether they are fixed or free (Fig. 21). It seems likely that the cause of this is the difference in surface properties of aggregate and steel. Rough surfaces provide more nucleation sites as compared to smoother surfaces and, further, the aggregate may absorb some water, which would reduce the local W/C.

d) Effect of Inclusion Content on Gap Formation

This is basically a comparison between the gaps formed in pastes, mortars, and concretes. It is important to note that the volume of aggregate (fine+coarse) was the same for mortar and concrete mixes. Only coarse aggregates were present in mortar specimens, which means that the concrete mixes have more fine particles than the mortars. The addition of aggregates to produce mortars and concretes led to smaller gaps. For example, a difference in gap width of 84% was observed in the case of silica fume paste and mortar specimens (refer to Figs. 9 and 21). On the other hand, for mortars and concretes, the difference was around 43%. A contrary result is given by the OPC only case with W/C=0.5, where there was actually an increase in gap size. From these observations, it can be said that aggregate content and grading may lead to reduced gap size, but more tests are needed to support this idea.

e) Effect of Chemical Admixtures

With regard to gap formation, the effect of a superplasticizer (SP) is also shown in Fig. 21 for silica fume-replaced systems. For the case of free inclusions, no gaps were observed. On the other hand, for fixed inclusions and for both mortar and concrete cases, almost all systems containing the superplasticizer indicated a slight increase in gaps width. However, this increase of at most 100 μm is not very significant and can be easily attributed to other factors. An in-depth investigation will be carried out regarding this matter.

7.3 Discussion of Transition Regions

The discussions above have focused on the gaps formed below the inclusions. Here, the difference between the matrices affected by the presence of inclusions is discussed. Figures 7 and 17 show microhardness results for the OPC series at 28 days for steel-paste and aggregate-paste ITZs, respectively. It is observed that for the case of a steel bar-paste ITZ, there is a steeper decrease in microhardness as the interface is approached in contrast with the aggregate case, where there is a more uniform distribution. From this it can be concluded that aggregate-paste transition regions are better than those of steel since the transition region microhardness in the former is not that different from that of the bulk matrix. In connection with the discussion of gap formation, this result might also be due to the fixed nature of the steel bars, the fact that the aggregate was present during mixing and free to move during casting, and the difference in surface conditions of the two types of inclusion.

8. CONCLUSIONS

This paper has demonstrated that there is a difference between aggregate-matrix and steel bar-matrix ITZs specifically with regard to the addition of mineral admixtures and gap formation. Incorporation of mineral admixtures reduced or inhibited gap formation in aggregate-matrix systems, while the addition of mineral

admixture resulted in large gaps below horizontal bars, in all but the fly ash case.

Further, the ITZs around aggregate particles are shown to be better than those around steel bars due to the narrower gaps or the absence of gaps and the more uniform microhardness distribution in the former. The ability of an inclusion to move during casting was shown to be a major factor contributing to gap formation.

Acknowledgment

The authors wish to express their most sincere gratitude to Prof. Shigeyoshi Nagataki, Prof. Kazuhiko Kawashima, Prof. Osamu Kusakabe, and Dr. Kazuo Tateishi for their helpful discussions. Special thanks are also extended to all members of the Concrete Laboratory for their help in the experiments. The support given by the Ministry of Education in making this study possible is also appreciated.

References

- [1] Farran, J., "Introduction: The transition zone - discovery and development", in *Interfacial Transition Zone in Concrete*, Maso, J. C., ed., E & FN Spon, London, 1996
- [2] Monteiro, P. J. M. and Mehta, P. K., "Ettringite Formation on the Aggregate-Cement Paste Interface", *CCR*, Vol. 15, pp. 378-90, 1985
- [3] Mehta, P. K., *Concrete: Materials, Structure and Properties*, Prentice-Hall Inc., 1986
- [4] Breton, D., Carles-Guibergues, A., Ballivy, G. and Grandet, J., "Contribution to the Formation Mechanism of the Transition Zone Between Rock-Cement Paste", *CCR*, Vol. 23, pp. 335-46, 1993
- [5] Scrivener, K. L. and Pratt P. L., "Characterization of Interfacial Microstructure", in *Interfacial Transition Zone in Concrete*, Maso, J. C., ed., RILEM Technical Committee 108-ICC Report, E&FN Spon (Chapman & Hall), 1996
- [6] Pinchin, D. J. and Tabor, D., "Interfacial Phenomena in Steel-Fibre Reinforced Cement I: Structure and Strength of Interfacial Region", *CCR*, Vol. 8, pp. 15-24, 1978
- [7] Barnes, B. D., "The Contact Zone Between Portland Cement Paste and Glass 'Aggregate' Surfaces", *CCR*, Vol. 8, pp. 233-44, 1978
- [8] Barnes, B. D., Diamond, S. and Dolch, W. L., "Micromorphology of the Interfacial Zone Around Aggregates in Portland Cement Mortar", *J. Am. Ceram. Soc.*, Vol. 62, No. 1-2, pp. 21-4, 1979
- [9] Scrivener, K. L. and Pratt, P. L.: *Proc.*, 8th ICCR, Rio, Vol. 111, pp. 466-71, 1986
- [10] Scrivener, K. L., Crumbie, A. K. and Pratt, P. L.: "A Study of the Interfacial Region Between Cement Paste and Aggregate in Concrete", in *Bonding in Cementitious Composites*, Mindess, S. and Shah, S. P., eds., Materials Research Society Symposium Proceedings, Vol. 114, 1988
- [11] Struble, L., "Microstructure and Fracture at the Cement Paste-Aggregate Interface", in *Bonding in Cementitious Composites*, Mindess, S. and Shah, S. P., eds., Materials Research Society Symposium Proceedings, Vol. 114, 1988
- [12] Scrivener, K. L. and Gartner, E. M., "Microstructural Gradients in Cement Paste Around Aggregate Particles", in *Bonding in Cementitious Composites*, Mindess, S. and Shah, S. P., eds., Materials Research Society Symposium Proceedings, Vol. 114, 1988
- [13] Bentur, A. and Odler, I., "Development and Nature of Interfacial Microstructure", in *Interfacial Transition Zone in Concrete*, Maso, J. C., ed., RILEM Technical Committee 108-ICC Report, E&FN Spon (Chapman & Hall), 1996
- [14] Odler, I. and Zurz, A., "Structure and Bond Strength of Cement-Aggregate Interfaces", in *Bonding in Cementitious Composites*, Mindess, S. and Shah, S. P., eds., Materials Research Society Symposium Proceedings, Vol. 114, 1988
- [15] Alexander, M. G., "Two Experimental Techniques for Studying the Effects of the Interfacial Zone Between Cement Paste and Rock", *CCR*, Vol. 23, pp. 567-75, 1993
- [16] Mindess, S., "Tests to Determine the Mechanical Properties of the Interfacial Zone", in *Interfacial Transition Zone in Concrete*, Maso, J. C., ed., RILEM Technical Committee 108-ICC Report, E&FN Spon (Chapman & Hall), 1996
- [17] Ollivier, J. P. and Massat, M., "The Effect of the Transition Zone on Transfer Properties of Concrete", in *Interfacial Transition Zone in Concrete*, Maso, J. C., ed., RILEM Technical Committee 108-ICC Report,

E&FN Spon (Chapman & Hall), 1996

- [18] Massaza, F., "Action of Environmental Conditions, in Interfacial Transition Zone in Concrete", Maso, J. C., ed., RILEM Technical Committee 108-ICC Report, E&FN Spon (Chapman & Hall), 1996
- [19] Mindess, S., "Interfaces in Concrete", in Materials Science of Concrete, Vol. 1, Skalny J. P., ed., Materials Research Society, 1989
- [20] Monteiro, P. J. M., Gjorv, O. E. and Mehta, P. K., "Microstructure of the Steel-Cement Paste Interface in the Presence of Chloride", CCR, Vol. 15, pp. 781-4, 1985
- [21] Wei, S., Mandell, J. A. and Said, S., "Study of the Interface Strength in Steel Fiber-Reinforced Cement-Based Composites", ACI Materials Journal, July-August 1986
- [22] Page, C. L. and Vennesland, O., "Pore Solution Composition and Chloride Binding Capacity of Silica Fume-Cement Pastes", SINTEF, STF A82025, The Norwegian Institute of Technology, NTH, Trondheim, 1982 as cited in ref. 17
- [23] Page, C. L., "Mechanism of Corrosion Protection in Reinforced Concrete Marine Structures", Nature, Vol. 258, Dec. 11, 1975